Revue Roumaine de Chimie, 34, 2, 635–648 (1989)

INVESTIGATIONS OF STRAINED S-B-S BLOCK COPOLYMERS WITH DILUTE ELASTIC NETWORKS*

N. STRIBECK, S. POLIZZI [a], P. BÖSECKE and H. G. ZACHMANN
Institut für Technische und Makromolekulare Chemie, Universität Hamburg
[a] Dipartimento di Chimica Fisica, Università degli Studi di Venezia

Received October 26, 1988

Spin cast films of one pure SBS and two oil extended SBS samples are observed under first cycle straining in the synchrotron radiation beam at HASYLAB. A scattering curve is extracted by intersecting the scattering pattern in drawing direction. This scattering curve is analyzed by fitting a one dimensional fibrillar two phase model. Essential to a fit with parameters of physical sense is the assumption of a least two components. One of the two main components is identified by fibrils containing PS cylinders orientated parallel to strain, the other by such containing cylinders orientated in cross direction. Splitting of cylinder orientation in the drawn state seems to be essential to the mechanical properties of the thermoplastic rubber, since only those cylinders orientated with their axis in the direction of strain are rigid while those orientated cross to drawing direction are yielding. The amount of cylinders alotted to each of the two components is varying as a function of the diluting agent and appears mainly to be influenced by topological parameters: the cylindrical particle dimensions within a two dimensional pseudo lattice cell of slightly varying dimenions in longitudinal and cross cylinder direction respectively. While paraffinic mineral oil dilution causes the cylinders length to decrease and thus improves cylinder orientability within the pseudo lattice cell, aromatic oil dilution increases the particles diameter. The results are compared with those of a preceding study, which allowed determination of the degree of phase separation by absolute SAXS and with first TEM micrographs.

1. INTRODUCTION

The main objective of this article is the presentation of our actual state of research in studying the morphology of a SBS three block copolymer and its oil diluted descendants under strain. Our main experimental method is small angle X-ray scattering (SAXS), and the study comprises absolute measurements of the samples SAXS in the undrawn state,[1] development of an adapted theory for the evaluation of the scattering patterns of the drawn samples,[2] a report on experimental method and on first results for samples under strain [3] and a comprehensive presentation and discussion of the fully evaluated scattering patterns.[4]

---

* Lecture presented at the 3rd National Congress of Chemistry, Bucharest, Romania, Sept. 22nd, 1988

Early in 1967 Hendus et al.[5] observed an originally isotropical scattering pattern from an SBS sample, that under strain deforms towards "a very narrow ellipse with an intensity accumulation of layer line character". Papers recently published on this subject [6,7,8] use sample films prepared by solvent casting. This procedure is known to yield a very perfect microstructure, as was shown by many authors using transmission electron microscopy (TEM). Thus the SAXS patterns of these samples are very detailed, showing many distinct reflections which are difficult to interpret. In the present paper we are dealing with sample films that are produced by our Romanian collaboration partners.[9,10] Their rapid spin casting process, far from equilibrium, is closer to technical processes like injection moulding and the general scattering pattern of these samples looks like the rather simple one described by Hendus et al. in 1967. For this type of pattern we were able to develop a new evaluation tool and to analyze the scattering patterns. Beyond that D. Hong made first electron micrographs of two of the samples that we additionally present here.

Blending of SBS block copolymers with typically 50 pph (parts per hundred parts of polymer) of a mineral oil fraction is of technological interest, since it is known to improve tensile strength of the product and processing capabilities.[6] This improvements cannot be obtained by the use of highly aromatic mineral oil fractions, so normally a light, mainly paraffinic/naphthenic mineral oil fraction is used. Although there is a lot of patent literature on this topic, we did not find papers on the morphology of oil extended grades of SBS copolymers except the ones of Ceauşescu et al.[7,8] Our collaboration partners by the use of rubber network theories, indirectly conclude that the PS particles in the sample diluted with 50 pph of paraffinic mineral oil should be closer to spherical shape than the ones in the undiluted sample.

2. EXPERIMENTAL

The base sample investigated is a poly(styrene)—poly(butadiene)—poly(styrene) three block copolymer with molecular weights $M_n = 80{,}800$ g/mole for the middle and $M_n = 21{,}200$ g/mole for each of the end blocks. A polymer film was spin cast from toluene solution. This base sample shall be referred to as "SBS". It was modified by blending 50 pph (parts per 100 parts of the polymer) of each a highly paraffinic/naphthenic and highly aromatic mineral oil fraction to the solution before spin casting (samples "P50" and "A50"). Synthesis [11] and sample preparation [10] were described elsewhere. The SAXS of the samples under first straining was measured at the Hamburg Synchrotron Radiation Laboratory (HASYLAB) and recorded with a two-dimensional detector (VIDICON). The experiment in detail was described in a previous publication on the undiluted sample.[3] For each positive and integer stretching ratio $\lambda = \varepsilon + 1$ a scattering pattern was accumulated for 60 s. In a second experiment the accumulation time after applying strain was chosen to be 5 s. This was the minimal time to get a sufficient signal/noise ratio with the VIDICON detector. By comparison between both experiments we took a first glance at creep of orientation and order.

Absolute SAXS measurements of the undrawn samples were performed with a Kratky camera using the moving slit method. TEM micrographs were obtained from cuts of ca. 100 nm thickness, stained with OsO_4. TEM measurements were carried out using a Japanese H-800 electron microscope at Yanshan research institute, Beijing, P. R. China, operated at 200 kV.

3. RESULTS AND DISCUSSION

3.1. Influence of Diluents on Phase Separation

Fig. 1 shows the electron density difference (contrast) $\Delta\rho_{OB}$ between the two phases of our base SBS sample diluted with various diluent oils as a function of the volume fraction of oil in the poly(butadiene) phase, v_{OB}. The value of 24 el/nm^3, obtained for the undiluted SBS, is far below the theoretical value for optimal phase separation (38 el/nm^3) (cf.[1]). It could be shown that the electron density of the paraffinic/naphthenic oil is close to that of pure PB and the electron density of the aromatic oil is close to that of pure PS. All kinds of oil mainly invade the PB phase. The curve for paraffinic mineral oil clearly shows that oil dilution improves phase separation and can be extrapolated towards the theoretical value of contrast for infinite dilution of the PB phase. Concerning aromatic oil dilution, interpretation is more difficult. The three samples that were investigated while straining are indicated in the figure.

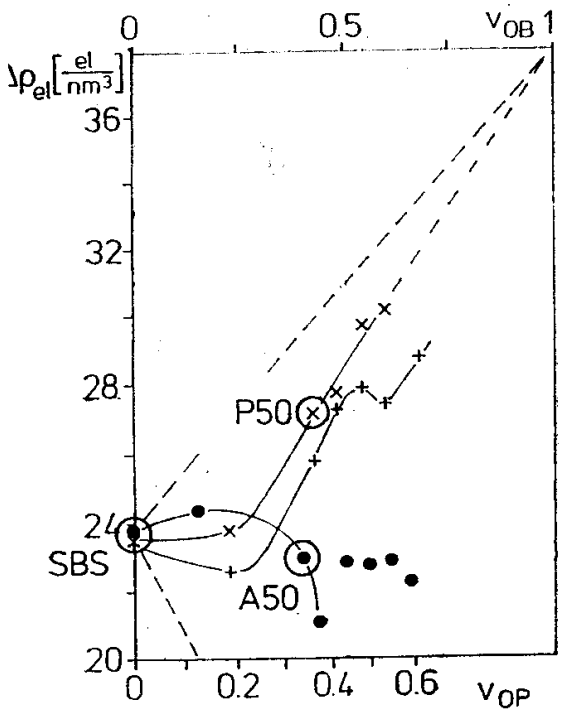

Fig. 1.— Contrast $\Delta\rho_{el}$ between the two phases of oil extended SBS three block copolymers as a function of v_{OB}, the volume fraction of oil in the PB phase for different kinds of diluents. (+): Low molecular weight PB (Lithene PM). (×): Paraffinic mineral oil fraction. (o): Aromatic mineral oil fraction

3.2. SAXS Results of Sample Straining

As an example the variation of the scattering pattern of SBS with elongation $\varepsilon = (l - l_0)/l_0$ and accumulation time after applying the additional strain is shown in Fig. 2. Here l_0 is the initial and l the actual length of the sample. Creep effect of the scattering pattern is visible, but too fast that it could be studied with the VIDICON detector and the experimental method chosen. Only for $\varepsilon = 1$ and 2 an effect of layer line straightening could be observed. Thus the study of creep phenomena would require an adapted experimental method and possibly a faster detector. For the further evaluation we decided to use the "relaxed" scattering patterns that were accumulated for 60 s.

The general type of the scattering pattern, in the simplest case, suggests a one dimensional model of fibrils containing cylindrical particles within. Due to the closed layer lines a correlation among cylinders belonging

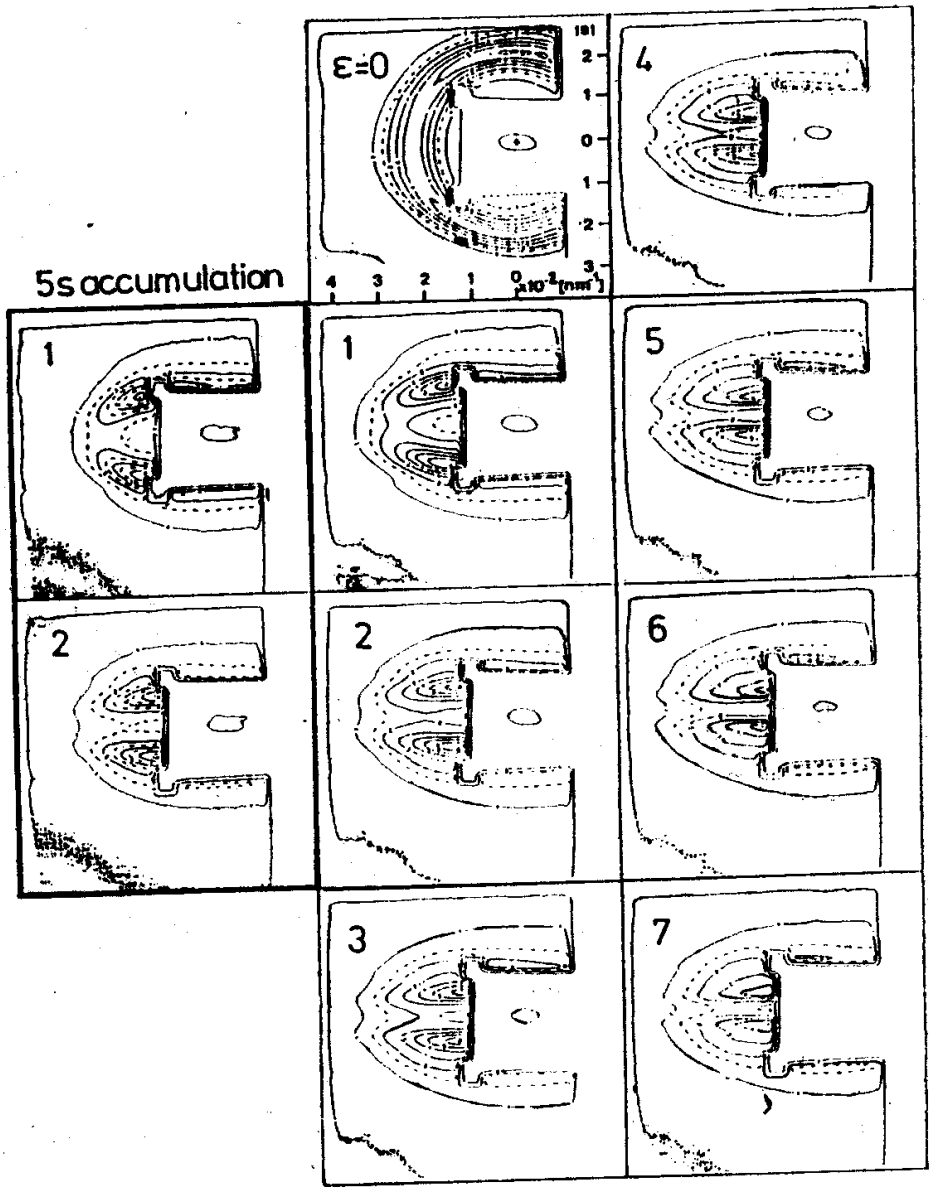

Fig. 2. — Variation of SAXS pattern with elongation ε and accumulation time after applying additional strain (60 s accumulation time to the right).

to different fibrils is not observable. In Fig. 3 the model and its parameters are visualized. d_1 and d_2 are the mean distances within phase 1 and phase 2 along the fibril. σ_1 and σ_2 are the variances of these distances and A_P is a weight parameter which is proportional to the number of cylinders contributing to the fibrillar model component and some other quantities. These five parameters in general are sufficient to describe the one dimensional fibrillar scattering curve $I_1(s)$, if the statistics how to build up the fibril is known. So we have two problems, namely to extract the one dimensional fibrillar scattering curve from the scattering pattern and to find out about the fibrillar statistics. It[1] was shown that one can extract the one dimensional scattering curve from the pattern by

taking the intersection of the pattern in the direction of draw. So we can take the curve along the s_3-component of the scattering vector in cylindrical coordinates, as is illustrated in Fig. 4. If one does not want

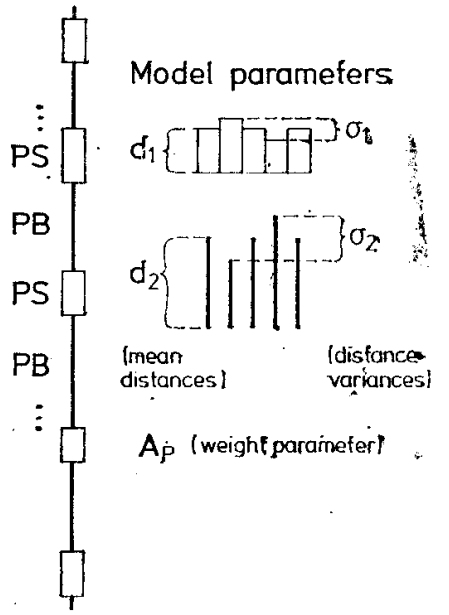

Fig. 3. — Illustration of a one dimensional fibrillar model and its parameters.

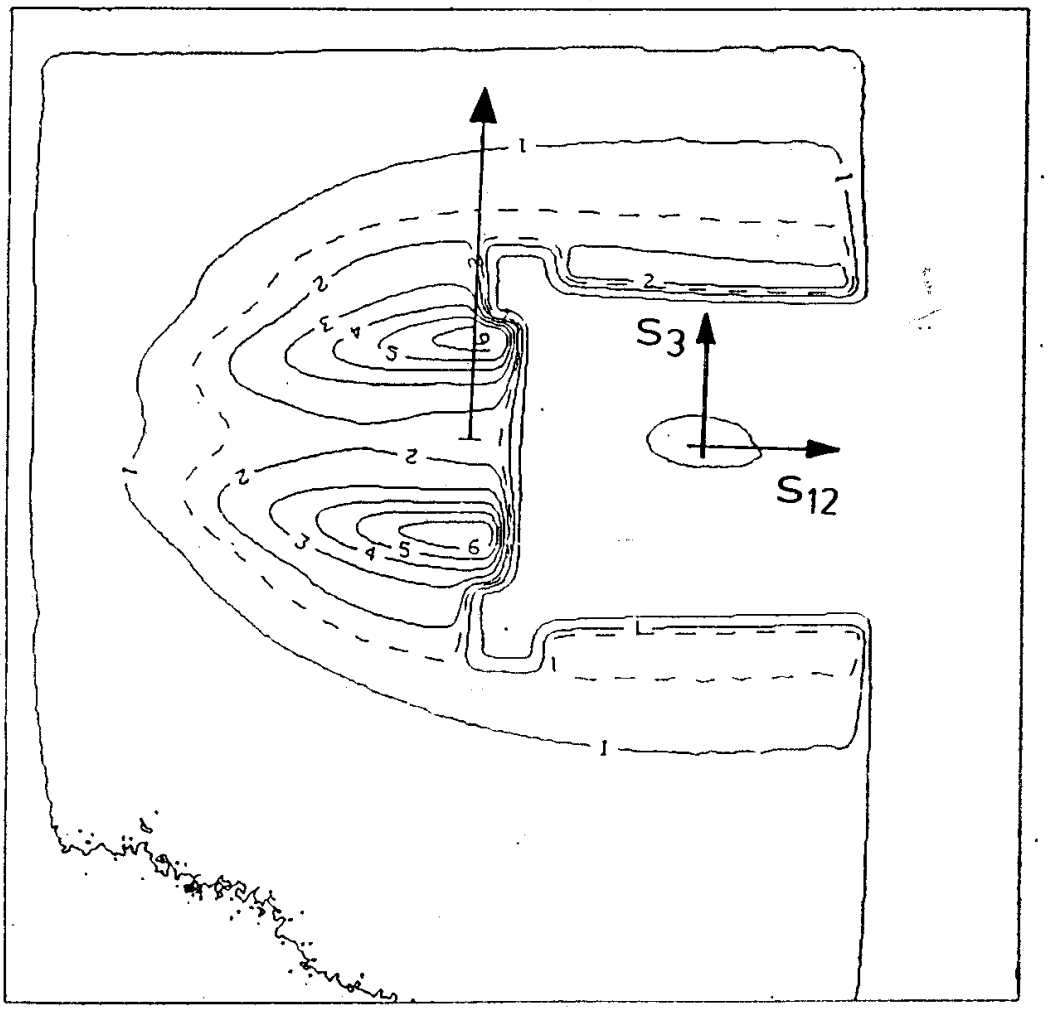

Fig. 4. — Illustration of intersecting the two dimensional SAXS pattern with cylindrical symmetry to get the one dimensional scattering curve $I_1(s^3)$. s_{12} and s_3 are the components of the scattering vector $\vec{s}$ in cylindrical coordinates.

to make assumptions on the fibrillar statistics, one can use a formula based on Rulands theory of interface distributions [12] and express the one dimensional scattering curve by an infinite sum over attenuated cosine terms :

$$I_1(s) = A_p/s^2 \cdot \left[1 - \sum_{i=1}^{\infty} w_i H_i(s)\right]$$

$$H_i(s) = \cos(2\pi\, d_i s) \cdot \exp(-2\pi^2 \sigma_i^2 s^2) \qquad (1)$$

Thus the increase of the σ_i with increasing i should give hints on the most probable statistical model. In doing the latter we found out that the assumption of one single fibrillar component was of no physical sense. After an initial increase the parameters σ_i dropped and again increased thereafter. To overcome this we had to assume the presence of a least two different kinds of fibrils. Anticipating the identification of the two main components from their parameters values and response to straining, we can illustrate them as is done in Fig. 5. In the cross component (left), the cylinders are lying cross to straining direction, while in the longitudinal component (right) they are oriented parallel to strain.

Scattering curves were fitted using a nonlinear regression algorithm. The quality of the fit was estimated by various tools derived in regression analysis theory. It turned out that the curves were best fitted either by a stacking model or by a lattice model for the one dimensional fibrillar statistics. Stacking statistics is the model with the poorer model inherent long range order.

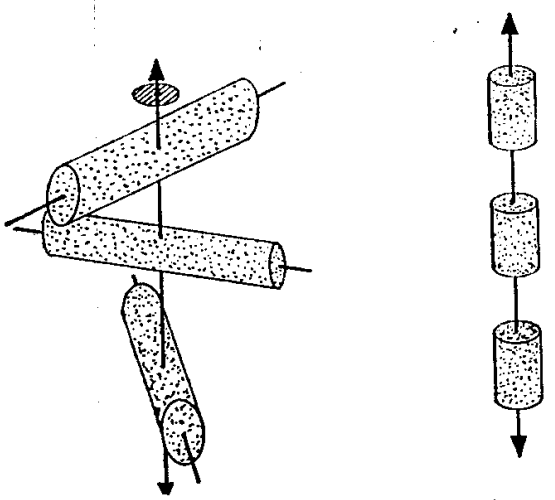

Fig. 5. — Illustrations of cross (left) and longitudinal (right) component fibrils. Cross component fibril shows the general case without correlation of orientation among the cylinders in the fibril.

The two main components for SBS and the A50 samples were found to be stacking statistics for all elongations. For the sample P50, diluted with paraffinic oil, this only is true for the elongations $\varepsilon = 1$ and $\varepsilon = 3$. For all the other elongations a double lattice model showed the smallest estimated error of the fit.

In the following the results of the three samples shall be presented by plotting the various model parameters versus the elongation ε. The individual parameter values and intervals of confidence will be shown by symbols with error bars. The height of the bar is chosen to mark a "2σ"-interval of confidence, assuming the error is normally distributed. I.e. the probability to find the true value of the parameter within the interval of confidence is 0.95. Considering the height of the error bars, smooth graphs are drawn through the points evaluated. Points without error bars have an error smaller than symbol height.

Because of the fact that the layer lines for all samples and $\varepsilon = 1$ are still somewhat bent, indicating imperfect orientation, it is not strictly allowed to apply our one dimensional model to these data. Therefore especially the weight parameters of this elongation should be interpreted cautiously. In the plots they are put in parenthesis. Furthermore bad model adaptation at $\varepsilon = 1$ in any case causes stacking statistics to fit better than the one dimensional lattice model, even if morphology really presents a lattice.

3.2.1. Pure SBS

Fig. 3 shows the distance parameters d_i from the double unidimensional model. The closed line graphs can be identified as the dimensions of hard particles, the PS-cylinders. The broken lines describe a weaker phase and shall be identified by the linear dimensions of the PB-matrix in the direction of strain. The first model is marked by triangles, the second by circles. Let us identify the triangle marked component by fibrils containing cylinders with their axis in the direction of strain (longitudinal component) and the circle marked component by fibrils with cylinders cross to drawing direction (cross component) and verify this identification by the response of its parameters to elongation and variation of oil dilution.

Looking at the closed line graphs, describing the PS-domains, it is obvious that the cylinders are rigid if orientated in longitudinal direction, while in cross direction they are weak and extend up to an elongation of $\varepsilon = 3$, where their dimension has increased from 22 nm to 60 nm. After this elongation the cross system fails, as can be seen from the following decrease of the mean radial dimension of the cross cylinders and the relaxation of the corresponding gap height. The strong increase of the gap in the longitudinal component denotes a takeover by this system. An extrapolation to $\varepsilon = 0$ is possible and leads to a cylinder height $h_c = 38$ nm and a diameter $d_g = 23$ nm. The initial heights of the gaps can be coarsely estimated, from an extrapolation in a plot $d_2(\varepsilon)/(\varepsilon + 1)$ vs. ε for the first three data points. The estimates result in a gap length of $d_g = 19$ nm for the longitudinal and $d_g = 42$ nm for the the cross component.

The weights A_P of both the longitudinal and cross component of the scattering under extension are given in Fig. 5. As one can see, the sum of the two main model weights is nearly constant from $\varepsilon = 3$. At low elongations an orientation effect can be observed : cylinders orientated indifferently at $\varepsilon = 2$ are comprised in the cross model. At $\varepsilon = 3$ they are oriented in longitudinal direction. In a middle range of ε a plateau for both weights is observable. The weight A_P is always proportional to the number of cylinders allotted to the component, but in such a plateau region even certain approximations should hold, allowing to assume the proportionality constants for both components to be the same. We recognize that the height of the plateau is identical for both main components and thus can state that about 50% of the cylinders can be oriented parallel to the direction of strain.

Double stacking statistics was found to be the model best fitted to data. From this we deduce, that the order of the superstructure is a poor one.

3.2.2. SBS Diluted with Paraffinic Oil

For the sample P50, Fig. 6 shows the dimensions d_g of the two phase system in drawing direction. As one can see, up to $\varepsilon = 3$ the PS particles of both the longitudinal and the cross component can be considered to be rigid. The extrapolation to $\varepsilon = 0$ yields cylinders of $d_g = 22$ nm and $h_c = 28$ nm. The initial heights of the gaps can be estimated, if one plots $d_2(\varepsilon)/(\varepsilon + 1)$ vs. ε for the first three data points and extrapolates towards zero. The estimates result in a gap length of $d_g = 35$ nm for both the longitudinal and the cross component.

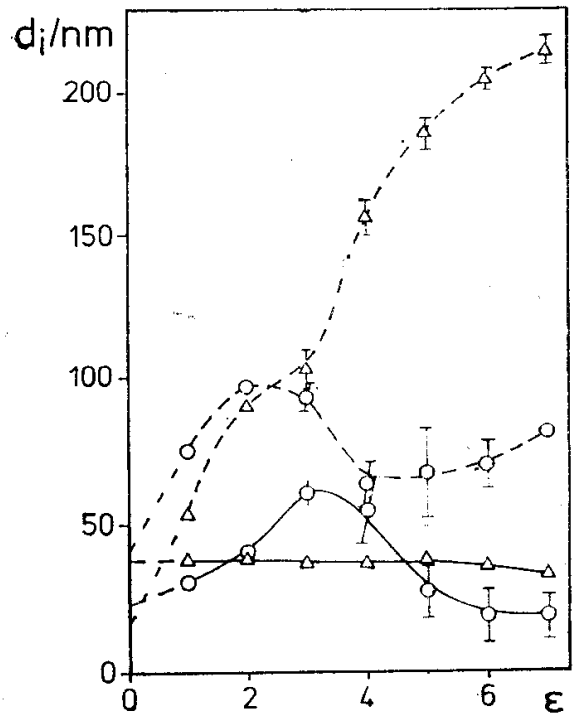

Fig. 6. — Dimension parameters d_i vs. elongation ε of pure SBS sample fitted with double fibrillar stacking statistics. (0): Fibrils with cylinders lying cross drawing direction. (Δ): Fibrils with cylinders orientated in drawing direction. Closed graphs: Cylinder dimensions (PS). Broken graphs: Gap dimensions (PB).

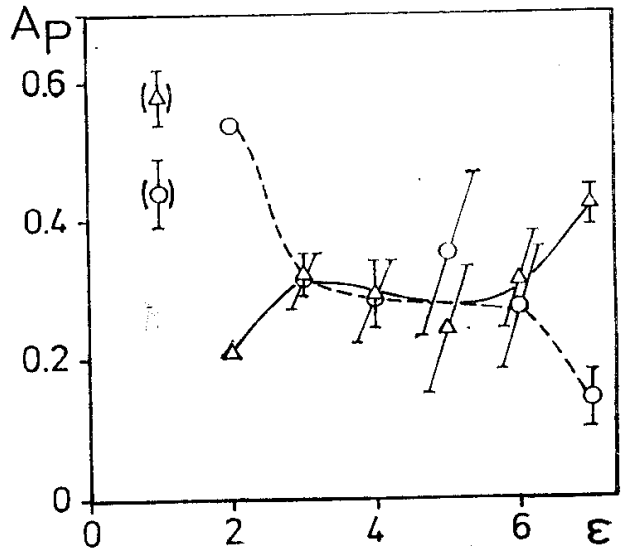

Fig. 7. — Weights A_p vs. elongation ε of pure SBS sample fitted with double fibrillar stacking statistics. (⊙): Component of fibrils with cylinders lying cross drawing direction. (Δ): Fibrils with cylinders orientated in drawing direction. Parenthesis for $\varepsilon = 1$ denotes poor model adaptation due to bent layer lines.

Near $\varepsilon = 4$ the cross cylinders begin to yield, with the cylinder diameter increasing up to 80 nm. Both matrix dimensions respond by relaxation to a constant value, further elongation advances by disruption of the cylinders lying cross to the direction of deformation, until again matrix material is elongated after $\varepsilon = 7$. At an elongation of $\varepsilon = 3$ the scattering curve is best fitted with a stacking model, which points to the fact that the instable state is inducing disorder to the morphology.

The following scattering curves again are lattice model fitted, but now in the cross component an inversion of the phase decorating the lattice has taken place. While at $\varepsilon = 2$ the curve was fitted best with a cross component in which the PS phase was decorating the lattice, from now on the PB matrix is forming the decoration. For the longitudinal component no such inversion of lattice decoration was observed.

Fig. 8 shows the development of the weights A_T as a function of elongation. The initial orientation effect can be observed until $\varepsilon = 3$, where the plateau is reached. In the plateau the amount of cylinders oriented parallel to strain is approximately 87 %.

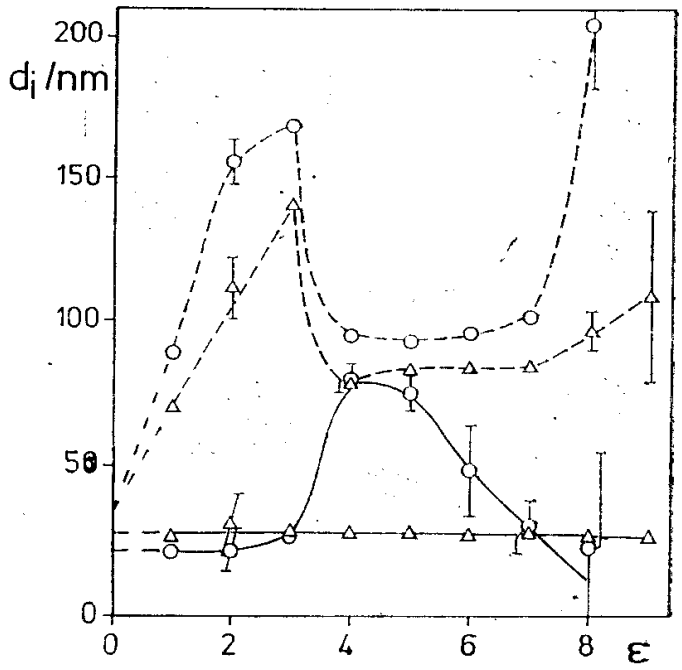

Fig. 8. — Dimension parameters d_i vs. elongation ε of P50 sample containing 50 pph of paraffinic oil. (⊖): Fibrils with cylinders lying cross drawing direction. (Δ): Fibrils with cylinders orientated in drawing direction. Closed graphs: Cylinder dimensions (PS). Broken graphs: Gap dimensions (PB).

Thus, paraffinic oil dilution decreases the cylinders anisotropy, helps the cylinders optimal orientation parallel to stress and in cross direction improves the relative hardness of the cylinders with respect to the matrix. Due to lattice model fit the morphology can be said to show a goad degree of order.

3.2.3. SBS Diluted with Aromatic Oil

For the sample A50 the response of the distances d_c to straining is plotted in Fig. 9. The cylinders orientated in the direction of strain are rigid again. Extrapolation of the cylinders height will be discussed in the next passage. The cylinders cross drawing direction, on the other hand, are flexible even at $\epsilon = 1$, so that no extrapolation to their initial thickness is possible. A very coarse estimate for the initial cylinder diameter and the gaps can be done the same way as for the preceding samples. The values are indicated in the plot. The cylinder diameter thus can be estimated by $d_c = 29$ nm and for the gap lengths we get values of $d_g = 19$ nm for the longitudinal and $d_g = 30$ nm for the cross component.

At $\epsilon = 5$ the cross system has failed and one finds a takeover by the longitudinal system, indicated by a sudden increase of as well PB anb PS mean distance. A similar behaviour was found in the undiluted SBS sample at an elongation of $\epsilon = 4$.

In Fig. 11 the weights A_P of the sample A50 are plotted. As one can see, the plateau is reached lately at $\varepsilon = 5$. Here the amount of the longitudinal component is very low while most of the cylinders contribute

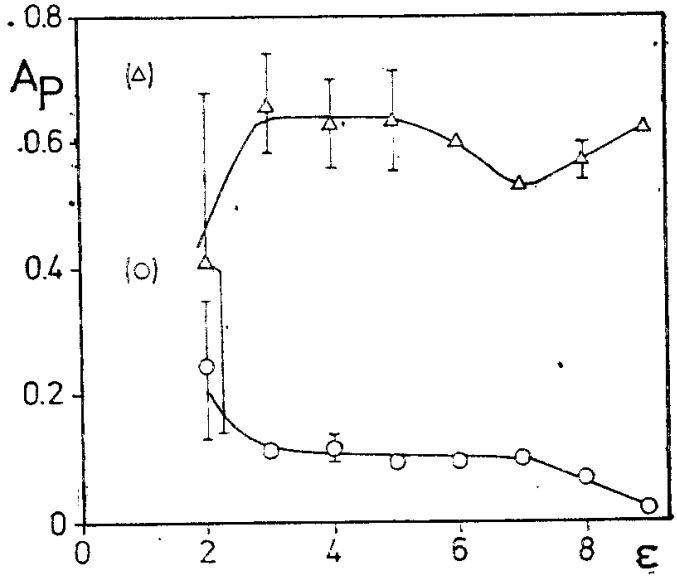

Fig. 9. — Weights A_P vs. elongation ε of P50 sample. (○) : Component of fibrils with cylinders lying cross drawing direction. (Δ) : Fibrils with cylinders orientated in drawing direction. Parenthesis for $\varepsilon = 1$ denotes poor model adaptation due to bent layer lines.

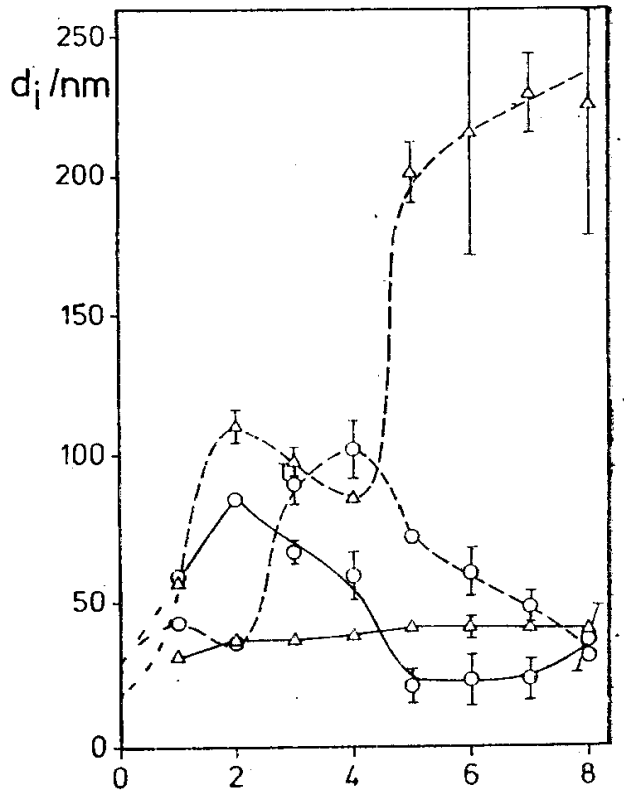

Fig. 10. — Dimension parameters d_i vs. elongation ε of A50 sample fitted with fibrillar stacking statistics. (○) : Fibrils with cylinders lying cross drawing direction. (Δ) : Fibrils with cylinders orientated in drawing direction. Closed graphs : Cylinder dimensions (PS). Broken graphs : Gap dimensions (PB).

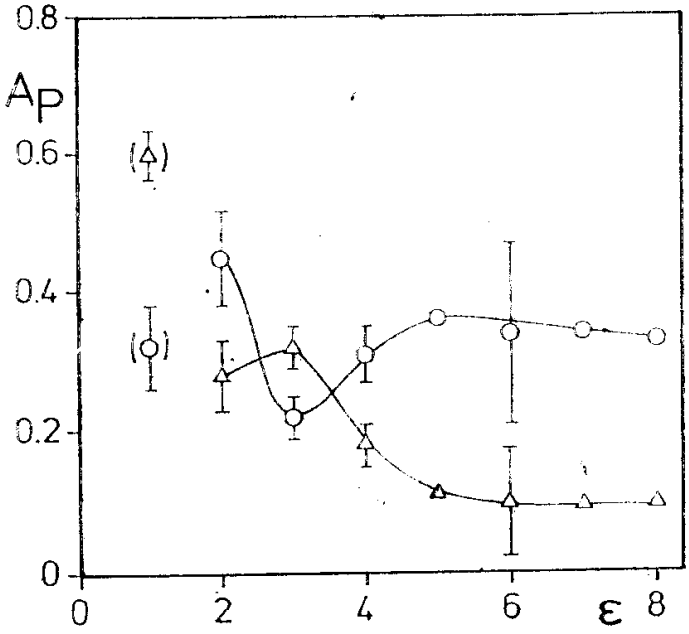

Fig. 11. — Weights A_P vs. elongation ε of A50 sample. (○) : Component of fibrils with cylinders lying cross drawing direction. (Δ) : Fibrils with cylinders orientated in drawing direction. Parenthesis for $\varepsilon = 1$ denotes poor model adaptation due to bent layer lines.

to the cross component. At $\varepsilon = 3$ there is a significant valley in the cross component that is accompanied by a peak in the longitudinal component. The peak coincides with the range of longitudinal fibril relaxation and the valley does so with the range of cross cylinder disruption. The explanation by an orientation phenomenon is supported by results of the variance (σ) plots, that are not presented in this paper. We assume that the increase of the longitudinal components amount is caused by a latent (and only fair) longitudinal orientation of a certain amount of cylinders at low elongations, so that the longitudinal component is increased. While cross cylinders under tension are disrupting, an orientation relaxation from longitudinal to cross orientation occurs, which can be observed in the decrease of the longitudinal component and the corresponding increase of the cross component between $\varepsilon = 3$ and 5. Thus we take the true cylinder height from high elongations and find $h_c = 14$ nm.

In the plateau, found at high elongations, approximately only 21 % of the cylinders are oriented parallel to strain.

Thus aromatic oil dilution slightly increases the cylinders height, hinders the optimal cylinder orientation parallel to stress and reduces the relative hardness of the cylinders lying cross to drawing direction. The morphology shows a low degree of order, as is true for the undiluted SBS.

3.3. Discussion of Extrapolated or Estimated Dimensions

In the preceding paragraphs we could extrapolate or estimate values for the mean dimensions of the particles and the mean distances between them in the undrawn state, which are compiled in Table 1.

As one can see, pure SBS shows a rather wide gap d_{gc} in cross direction between neighbouring cylinders. Anticipating a look at the corresponding electron micrograph, we interpret this as an effect of bad phase separation (see [1]): Imperfect PS "particles" between the more stable cylinders that are even vanishing at a very low elongation. So in d_{gc} we just estimate the mean PB distance between two more stable cylinders, "blended" with some additional imperfect PS material.

Paraffinic oil dilution only affects the cylinder height, while aromatic oil dilution mainly seems to influence the cylinder diameter. Both diluents cause a reduction of the h_c/h_c-ratio of the cylinders, but parafinic oil dilution decreases the cylinder height, while aromatic oil dilution seems to increase the cylinder diameter.

If we trust in the estimated values for the mean initial distances between the cylinders, the result on the particle dimensions can even be generalized. From the values in Table 1 we construct nearly the same "pseudo lattice cell" for P50 and A50 (see Fig. 14). The lattice cell of pure SBS appears only somewhat wider in cross

Table 1

Extrapolated or estimated (*) values for the cylinder dimensions and the distances in between for the undrawn state h_c, d_c: cylinder height and diameter. d_{gl} d_{gc}: gaps in longitudinal and cross direction (with respect to the cylinder axis)

	SBS	P50	A50
h_c/nm	38	28	41
d_c/nm	23	22	*23
d_{gl}/nm	*19	*35	*19
d_{gc}/nm	*42	*35	*30

cylinder direction. A result compatible with this was found in a preceding work on the unstretched samples : a long period nearly constant for three kinds of diluents and oil dilutions up to 140 pph.[1].

Thus a reasom for the different a mount of cylinders allotted to each of the two components with different cylinder orientation is obviously

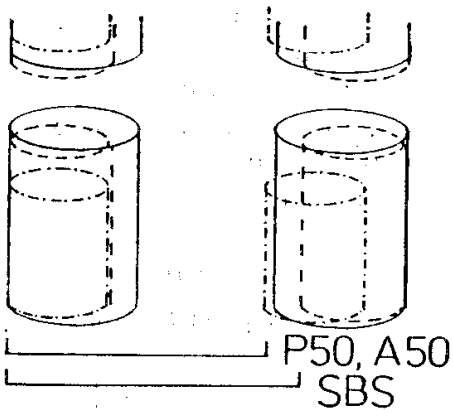

Fig. 12. — Pseudo lattice cells containing cylindrical particles constructed from extrapolated or estimated dimensions for the undrawn state. Broken line : Pure SBS. Dashed and dotted line : Sample P50, 50 pph paraffinic oil dilution. Full line : Sample A50, 50 pph aromatic oil dilution. Decrease of lattice constants cross component on oil dilution is indicated.

given by topology : the cylindrical particles dimensions within a pseudo lattice cell of nearly constant extent, determining the particles possibility to rotate and follow an external torque.

3.4. TEM Micrographs

In fig. 13 the first two electron micrographs obtained from SBS and a sample diluted with 60 pph of paraffinic oil (P60) are presented. The PS particles appear light, while the PB phase, due to staining, is the darker one. As one can see, the results of our SAXS study are excellently verified by the TEM pictures.

Bad phase separation of SBS is visible by the comparatively bad staining of the interstices, meaning a pollution of the PB phase by poly (styrene). The microstructure is rather a chaotic one, which is in agreement to the stacking model fit of the sample.

Measurements of the cylinder dimensions and the distances between them in well developed regions resulted in the same values that were found by the SAXA pattern analysis for the samples SBS and P50, which is very close to P60 sample.

Looking at the topology of P60, one finds clusters of ordered cylinders, built up from few cells of lattice character. The cells contain one cylinder in the middle that is surrounded by 5 to 8 other cylinders, the most frequent number being 6. Thus we recognize a disturbed hexagonal lattice structure.

4. OUTLOOK

The results of this work show that using an adapted theoretical approach and model for the evaluation of the small angle X-ray scattering can give profound information on the two phase topology of an (oil diluted) SBS block copolymer not only in the drawn state.

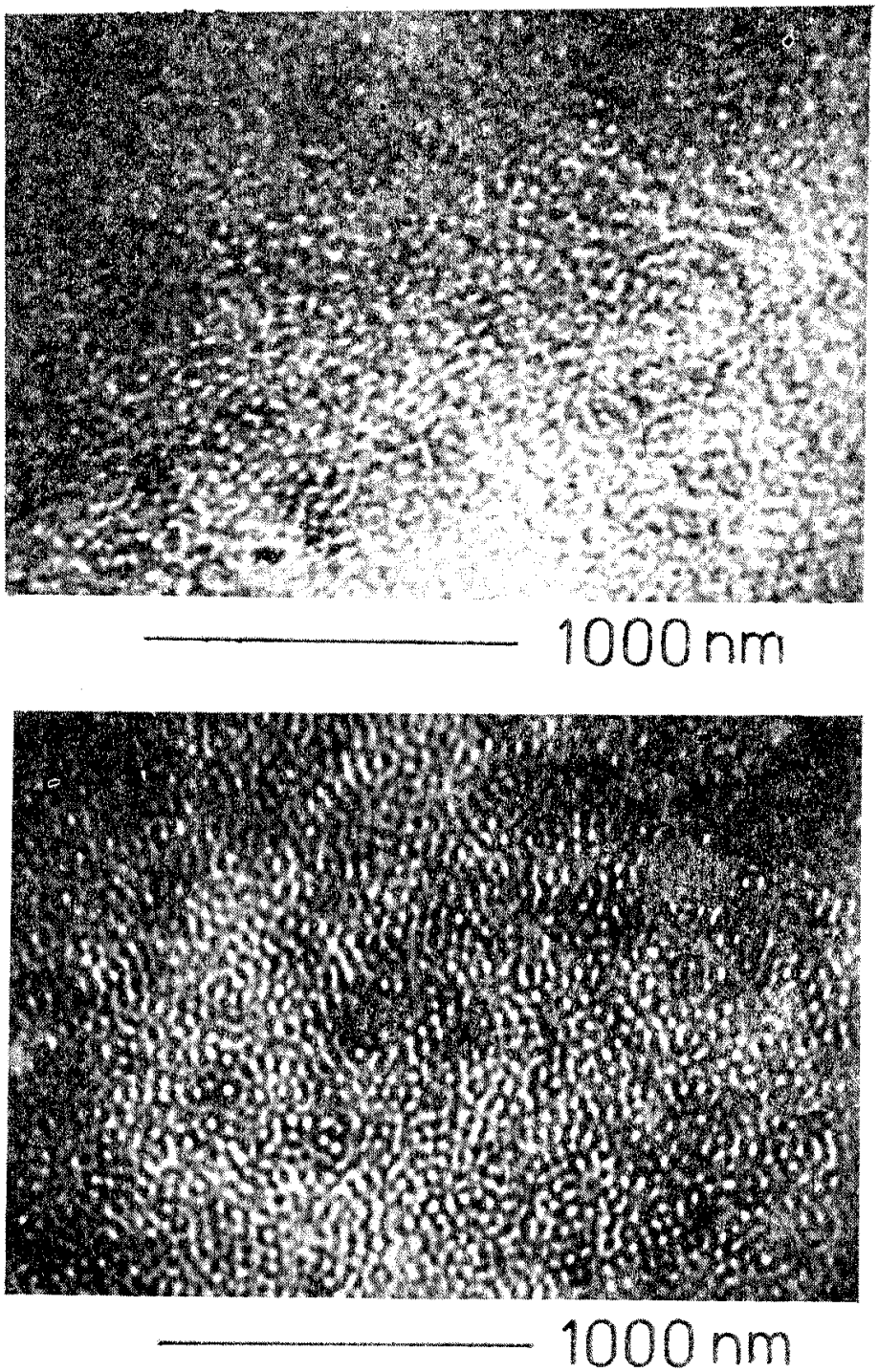

Fig. 13. — TEM micrographs of pure SBS (above) and P60 (SBS + 60 pph of paraffinic mineral oil, below). Length of the bars : 1000 nm.

After having studied linear three block copolymers, it will be interesting to investigate diluted SBS star block copolymers. These types are more frequently used than the linear ones. Also resin diluted SBS block copolymers are of interest for the production of adhesives and thus could be studied.

Creep could be studied in an adapted experiment : samples could rapidly be strained from their initial length to a medium elongation

($\varepsilon \cong 2$) and variation of the scattering curve in the direction of strain could be recorded rapidly, if a fast diode array detector were used.

The effect of oil dilution to the relaxed morphology could be studied by further TEM investigations.

As noted in the discussion to the lecture, changes of the PS domain dimensions could have occurred between preparation and measurements (more than 1 year, samples kept at room temperature) due to thermal aging.

REFERENCES

[1] S. Polizzi, et al., (1988) submitted to *Colloid Polym. Sci.*
[2] N. Stribeck (1988) submitted to *Colloid Polym. Sci.*
[3] S. Polizzi, et. al., (1988) submitted to *Polymer.*
[4] N. Stribeck, et. al., (1988) submitted to *Colloid Polym. Sci.*
[5] H. Hendus, et. al., *Colloid Polym Sci.*, **216**, 110—119, (1967).
[6] R. Séguéla and J. Prud'homme, *Macromolecules*, **21**, 635—643 (1988).
[7] T. Pakula, et. al., *Macromolecules*, **18**, 1294—1302, (1985).
[8] R. W. Richards and J. T. Mullin, *Mat. Soc. Symp. Proc.*, **79**, 299—308, (1988).
[9] E. Ceaușescu, et. al., *Rev. Roumaine Chim.*, **28**, 299—323, (1983).
[10] E. Ceaușescu, et. al., *Pure Appl. Chem.*, **56**, 319—328 (1984).
[11] In : E. Ceaușescu (ed) "Forschungen im Bereich der Chemie und Technologie der
[1] Polymere. Birkhäuser, Basel, 1986", pp. 65—77.
[2] W. Ruland, *Colloid Polym. Sci.*, **255**, 417—427 (1977).